NASA TM X-73,067

NASA TECHNICAL MEMORANDUM

NASA TM X-3213

APPLICATION OF NUMERICAL OPTIMIZATION TO THE DESIGN OF LOW-SPEED AIRFOILS

Raymond M. Hicks and Garret N. Vanderplaats

Ames Research Center

Moffett Field, Calif. 94035

NATIONAL AERONAUTICS AND SPACE ADMINISTRATION • WASHINGTON, D. C. • MARCH 1975

1. Report No.	2. Government Accession No.	3. Recipient's Catalog No.
NASA TM X-3213		

4. Title and Subtitle	5. Report Date
APPLICATION OF NUMERICAL OPTIMIZATION TO THE DESIGN OF LOW-SPEED AIRFOILS	March 1975
	6. Performing Organization Code
7. Author(s)	8. Performing Organization Report No.
Raymond M. Hicks and Garret N. Vanderplaats	A-5863
	10. Work Unit No.
9. Performing Organization Name and Address	505-10-12
Ames Research Center, NASA Moffett Field, Calif. 94035	11. Contract or Grant No.
	13. Type of Report and Period Covered
12. Sponsoring Agency Name and Address	Technical Memorandum
National Aeronautics and Space Administration Washington, D. C. 20546	14. Sponsoring Agency Code

15. Supplementary Notes

16. Abstract

A practical procedure for the optimum design of low-speed airfoils is demonstrated. The procedure uses an optimization program based on the method of feasible directions coupled with an aerodynamic analysis program that uses a relaxation solution of the inviscid, full potential equation. Results are presented for airfoils designed to have small adverse pressure gradients, high maximum lift, and low pitching moment.

17. Key Words (Suggested by Author(s))	18. Distribution Statement
Wings Airfoil General aviation	Unclassified – Unlimited STAR Category – 02

19. Security Classif. (of this report)	20. Security Classif. (of this page)	21. No. of Pages	22. Price*
Unclassified	Unclassified	28	$3.75

*For sale by the National Technical Information Service, Springfield, Virginia 22151

NOTATION

a_i design variables for upper surface $i = 1, 6$ (coefficients used in the expression for upper surface ordinates)

b_i design variables for lower surface $i = 1, 6$ (coefficients used in the expression for lower surface ordinates)

c chord

C_D section drag coefficient

C_L section lift coefficient

C_m section pitching-moment coefficient

C_p pressure coefficients, $(p_1 - p)/q$

$G(\bar{x})$ constraint function

M Mach number

$NCON$ number of constraint functions

OBJ objective function

p free-stream static pressure

p_1 local static pressure

P_i Legendre polynomials ($i = 1,6$)

q free-stream dynamic pressure

RN Reynolds number

$\bar{s}$ move direction vector

t thickness

ΔTE trailing-edge thickness

V area within airfoil contour

x chordwise distance

$\bar{x}$ vector of design variables

y vertical distance

α angle of attack

β movement in s direction

Subscripts

ℓs lower surface

max maximum

min minimum

us upper surface

APPLICATION OF NUMERICAL OPTIMIZATION TO THE DESIGN OF LOW-SPEED AIRFOILS

Raymond M. Hicks and Garret N. Vanderplaats

Ames Research Center

SUMMARY

A practical procedure for the optimum design of low-speed airfoils is demonstrated. The procedure uses an optimization program based on the method of feasible directions coupled with an aerodynamic analysis program that uses a relaxation solution of the inviscid, full potential equation. The analysis program is valid for both incompressible and compressible flow thereby making optimum design of high-speed airfoils also possible. Results are presented for the following three different constrained optimization problems at fixed angle of attack and Mach number: adverse pressure gradient minimization, pitching moment minimization, and lift maximization. All three problems were studied with various aerodynamic and geometric constraints.

INTRODUCTION

The design of advanced general aviation aircraft has indicated a need for a wider choice of airfoil sections to meet the increased requirements of safety, utility, performance, and economy to operate in the complex environment of today's air transportation system. More airfoil sections could be provided by systematic variation of airfoil parameters through wind-tunnel testing or by the development of advanced computer programs to calculate section aerodynamic characteristics. It was felt that the general aviation manufacturers would be better served by the latter approach, that is, the development of a simple, direct approach to airfoil design since a modern family of airfoils would not necessarily meet the requirements of a particular design problem. The goal has been to develop a method that would allow the aircraft designer to calculate airfoil contours so that the requirements of the design could be met without the inevitable compromise that arises when an airfoil must be chosen from an existing family of sections. Achievement of this goal has been enhanced by the rapid advancement in aerodynamic and numerical optimization programs over the last few years. Aerodynamic coefficients, pressure distribution, boundary-layer transition, and even flow separation can now be predicted for two-dimensional sections. Hence, it is now possible to design an airfoil on a computer.

Considerable effort has been expended within NASA, the universities, and industry over the last few years to develop methods that can be used to design advanced low-speed airfoils (e.g., refs. 1 and 2). Such methods have been used in both the direct and inverse modes to design airfoil sections (refs. 3–5).

In the direct mode, airfoil design has been mainly intuitive combined with wind-tunnel tests to enhance the design process. Inverse methods have been used successfully to design airfoils for

specific flight conditions but have the disadvantage of requiring an a priori knowledge of the desirable form of the pressure distribution before the design is attempted. While such knowledge may be available in some cases, the designer usually knows more about the required thickness, volume, trailing-edge angle, etc., than about the required velocities or pressures over the airfoil surfaces. Because of the inadequacies of current design methods, a practical engineering procedure based on numerical optimization which allows the designer to specify geometric requirements of the airfoil at the start of the design is under development at Ames. Both low-speed and high-speed airfoil sections can be designed with this method. This method was shown to be both practical and easy to use for the design of shock-free transonic airfoils (ref. 6). The technique has been applied here to the design of potential general aviation airfoils.

The results presented must be considered preliminary and are intended only to illustrate the usefulness and simplicity of the technique.

DESIGN METHOD

The design method demonstrated here used two existing computer programs – an optimization program based on the method of feasible directions (ref. 7) and an aerodynamic analysis program based on a relaxation solution of the full potential equation (ref. 8). The technique is applicable to both subsonic and transonic flow. The theoretical bases for both computer programs are discussed briefly in the appendix.

The thickness distributions of the airfoils considered are given by

$$y_{us} = a_1\sqrt{(x/c)} + a_2(P_2 + 1) + a_3(P_3 - 1) + a_4(P_4 + 1) + a_5(P_5 - 1) + a_6(P_6 + 1)$$

$$y_{\ell s} = b_1\sqrt{(x/c)} + b_2(P_2 + 1) + b_3(P_3 - 1) + b_4(P_4 + 1) + b_5(P_5 - 1) + b_6(P_6 + 1)$$

where y_{us} and $y_{\ell s}$ are the upper- and lower-surface ordinates, respectively, and $P_2, \ldots, P_6$ are Legendre polynomials given by

$$P_2 = 2(x/c) - 1$$

$$P_3 = 6(x/c)^2 - 6(x/c) + 1$$

$$P_4 = 20(x/c)^3 - 30(x/c)^2 + 12(x/c) - 1$$

$$P_5 = 70(x/c)^4 - 140(x/c)^3 + 90(x/c)^2 - 20(x/c) + 1$$

$$P_6 = 252(x/c)^5 - 630(x/c)^4 + 560(x/c)^3 - 210(x/c)^2 + 30(x/c) - 1$$

The square root term allows a blunt leading edge and assures matching of upper-surface and lower-surface derivatives of all orders at the leading edge. The coefficients $a_1, \ldots, a_6$ and $b_1, \ldots, b_6$ are the design variables perturbed by the optimization program to achieve optimum design.

Legendre polynomials were used to represent the airfoil geometry because optimization algorithms work more efficiently when orthogonal expressions are used. This particular representation of the airfoil geometry is not unique, and other forms such as Fourier series, piecewise polynomials, or other orthogonal polynomials are certainly possible choices. Optimum design problems were also solved using one expression for thickness and another for camber; however, the geometric representation used here was found to be more efficient for optimization because the upper and lower surfaces were not mathematically coupled.

All airfoils were constrained to have no negative thickness ($t \geqslant 0$) and to have a trailing-edge thickness no greater than 1 percent of the chord ($\Delta TE \leqslant 0.01c$). Unless otherwise noted, all design variables ($a_1, \ldots, a_6; b_1, \ldots, b_6$) were used for each optimization problem. All pitching-moment coefficients calculated during this study were referenced to the quarter chord. The parameter V (indicated in the figures) is the area contained within the contour of the normalized airfoil and can be considered a measure of the volume of a finite wing using the airfoils shown.

Some of the airfoils developed during this study may exhibit minor imperfections (e.g., reflexed curvature). No attempt was made to eliminate such minor flaws since the primary purpose of this effort was to demonstrate a technique rather than to finalize the design of specific airfoils. In an actual design, any surface irregularities could easily be eliminated by additional constraints on the airfoil geometry or by selecting an alternate expression for the thickness distribution.

In optimization problems of the type considered here, a starting airfoil is needed. Unless otherwise noted, the initial airfoil used here was obtained by fitting the thickness equations given above to six points on the upper surface and six points on the lower surface of the NACA 64_1–212.

DESIGN RESULTS AND DISCUSSION

The following numerical optimization problems, subject to geometric and aerodynamic constraints, were considered: adverse pressure gradient minimization, pitching moment minimization, and lift maximization.

The aerodynamic analysis program used here is applicable to inviscid flow only, hence drag minimization problems were not considered. However, a comparison of the inviscid optimization results with viscous calculations shows that many interesting design problems can be treated by an inviscid theory. In the near future, the optimization program will be coupled with a viscous aerodynamic analysis program, thereby permitting the consideration of drag during the optimization process.

The first problem considered here was the design of airfoils for high maximum lift coefficient. Since reliable methods are not available to accurately calculate $C_{L_{max}}$ and because of the close

relationship of $C_{L_{max}}$ to the shape of the upper-surface pressure distribution, airfoils that have small upper-surface pressure peaks and low adverse pressure gradients were developed.

Minimization of Adverse Pressure Gradient

The absolute value of the difference in pressure coefficients at $x/c = 0.003$ and $x/c = 0.2$ was taken as a measure of the upper-surface pressure gradient near the leading edge for the series of optimization problems considered here (i.e., the minimum value of $\left|C_{p_{us}}(x/c = 0.003) - C_{p_{us}}(x/c = 0.2)\right|$ was sought). The choice of this pressure difference as a measure of the pressure gradient is arbitrary and other quantities such as peak pressure coefficient could have been used.

The minimization of the upper-surface adverse pressure gradient at $M = 0.1$ and $\alpha = 6°$, subject to constraints on thickness and trailing-edge bluntness, is shown in figure 1. Note that when the adverse pressure gradient was reduced, a loss in lift occurred. Also, a modest "humping" of the pressure distribution between the leading edge and $x/c = 0.2$ occurs. However, this may not be undesirable since a favorable pressure gradient is achieved in the region of large curvature near the leading edge where the fluid particles are subjected to large centrifugal forces. Hence leading-edge stall may be eliminated. The final airfoil in figure 1 exhibits greater volume and smaller nosedown pitching moment.

Adverse pressure gradient minimization subject to constraints on pitching-moment coefficient, lift coefficient, and airfoil volume along with the thickness and trailing-edge constraints for $\alpha = 6°$ is shown in figures 2, 3, and 4. When the volume is required to be greater than or equal to a specified value ($V \geqslant 0.075$), the final airfoil is considerably thicker than the initial airfoil (fig. 2). Note the substantial reduction in pressure peak and adverse pressure gradient near the leading edge on the upper surface accompanied by an increase in volume of nearly 51 percent. Here, the constraint on lift coefficient prevented the loss in lift noted in figure 1. All constraints were satisfied by the final design. When the volume is constrained from above and below ($0.075 \leqslant V \leqslant 0.09$, fig. 3, or $0.075 \leqslant V \leqslant 0.08$, fig. 4) along with constraints on C_m, C_L, thickness, and trailing-edge bluntness, the final airfoils are considerably thinner but still exhibit small adverse pressure gradients near the leading edge on the upper surface (figs. 3 and 4). The improved pressure gradient results from an increase in the upper-surface ordinates near the leading edge (figs. 1 to 4). Increasing ordinates in this region eliminates leading-edge stall and increases the maximum lift coefficient by delaying flow separation to greater angles of attack (refs. 4, 9, and 10). Note that the final lift coefficient is greater for the thinner sections (figs. 3 and 4) than for the thick section in figure 2.

The effect of increasing the design angle of attack from 6° to 10° on minimization of adverse pressure gradient is shown in figure 5. The pressure peak is increased from −8.21 to −3.4 accompanied by a substantial reduction in the leading-edge adverse pressure gradient. Again a large increase in the upper-surface ordinates particularly near the leading edge was required to achieve the desired result. All constraints were satisfied by the final contour and the lift and pitching-moment coefficients were improved. While the final airfoil may achieve a large maximum lift coefficient, a drag penalty would probably be found at low lift. Drag will be explored experimentally during future wind-tunnel tests, and also theoretically when a suitable viscous aerodynamic program is available (the program is currently under development).

A superposition of the airfoils designed for angles of attack of 6° and 10° is shown in figure 6. The slight irregularity in the upper surface of the airfoil designed for $\alpha = 10°$ could easily be eliminated by imposing additional constraints on thickness and/or curvature.

Minimization of Pitching Moment

Pitching-moment minimization at $M = 0.1$ and $\alpha = 0°$ subject to constraints on thickness and trailing-edge bluntness is shown in figure 7. Note that the pitching-moment coefficient was reduced to zero along with a loss in lift. This result was achieved primarily by unloading the trailing edge along with a slight change toward a more symmetrical airfoil. The lower-surface pressure coefficients are less than those for the upper surface aft of the 75-percent chord station.

Pitching-moment minimization at $\alpha = 6°$ subject to thickness and trailing-edge bluntness constraints is shown in figure 8. Again the moment coefficient is reduced to near zero accompanied by a loss in lift by unloading the trailing edge of the airfoil. Before considering the more important problem of moment minimization subject to aerodynamic constraints along with more rigid geometric constraints, it was deemed appropriate to calculate the aerodynamic characteristics of the final airfoil in figure 8 by a viscous theory to explore the usefulness and practicality of design by an inviscid theory. Figure 9 compares the inviscid calculations with viscous calculations, where the agreement between the theories for pressure distribution, lift coefficient, and moment coefficient is good. This comparison indicates that useful low-speed design can be achieved with an inviscid theory so long as the drag of the final design is checked with a viscous theory or experimentally. (The viscous theory used here was not coupled with the optimization program for airfoil design because of the long computer time required for each calculation. The theory is described in reference 1.) Viscous and inviscid calculations are compared further later.

Moment minimization subject to constraints on lift coefficient, thickness, and trailing-edge bluntness is shown in figure 10. In this case, very little improvement in moment coefficient was realized. The reason for this lack of improvement is that the change in the design variables (coefficients $a_1, \ldots, a_6$ and $b_1, \ldots, b_6$ of the thickness equations) required to reduce the nosedown pitching moment is opposite the design variable change required by the lift constraint. Hence little can be done to improve the pitching moment without violating the lift constraint. Three possible solutions to this difficulty are: (1) Use a different equation to represent the airfoil geometry since cambered airfoils with forward loading are apparently difficult to achieve with the geometric equations used here. (2) Impose more constraints on the design. (3) Use a different initial airfoil.

Increasing the number of constraints was found to increase the probability of finding an optimum design during the study reported in reference 6; hence more constraints were used here. When additional constraints are imposed, the design is "pushed" in a different direction, which often improves the result, particularly if relative minimums are present. Constraints on upper-surface pressure gradient and volume were added and the design was rerun on the computer (fig. 11). The final airfoil exhibits nearly a 50-percent decrease in nosedown moment along with increased lift and volume and a reduced adverse presence gradient near the leading edge on the upper surface. So, again, imposing additional constraints is beneficial in the optimum design of airfoil sections.

Since the pitching moment was still not reduced to zero in the above example, a different initial airfoil was chosen for the next series of moment minimization problems. The initial airfoil used was a cambered version of a shock-free section developed during the study reported in reference 6. The results in figures 12, 13, and 14 show the effect of moment minimization subject to thickness and trailing-edge bluntness constraints only. Figures 13 and 14 show, respectively, the effect of changing the upper-surface and lower-surface design variables independently. In all three cases (figs. 12 to 14) the nosedown moment was reduced to near zero along with a reduction in lift coefficient. The pitching moment and lift reduction was achieved by generating a more symmetrical airfoil and unloading the trailing edge. The effect of adding a constraint on lift is shown in figure 15. In this case, the pitching moment was reduced by more than 50 percent along with a small decrease in lift and a substantial increase in volume. However, a moment coefficient of zero was still not achieved. In the future, alternate equations for the airfoil geometry will be used in an effort to achieve greater flexibility in design and hence easier attainment of the optimum.

Maximization of Lift

The same initial airfoil as used for the pitching-moment minimization results described previously (figs. 12 to 15) was used for all lift maximization problems except the final design problem. Lift maximization at $M = 0.1$ and $\alpha = 6^\circ$ subject to constraints on pitching moment, volume, thickness, trailing-edge bluntness, and upper-surface pressure coefficient at one chordwise station is shown in figure 16 (the arrow shows the position of the pressure coefficient constraint). The upper-surface pressure coefficient was constrained so that the peak upper-surface velocity and adverse pressure gradient could be reduced. The final airfoil exhibits nearly a 12-percent increase in lift along with a greater nosedown moment, a greater volume, and a smaller adverse pressure gradient. All constraints were satisfied by the final design.

The effect of increasing the moment constraint and moving the constraint on the upper-surface pressure coefficient forward is shown in figure 17. A smaller increase in lift was achieved than for the design shown in the previous figure primarily because of the "stronger" constraint on moment. Again, within the limits of the equation for geometry used here, reducing the pitching moment usually causes a decrease in lift. A further increase in pitching-moment constraint and an additional constraint on lower-surface pressure coefficient produced a final airfoil with nearly the same lift as the initial airfoil (fig. 18). The additional constraint on lower-surface pressure coefficient at the 65-percent chord station was imposed to smooth the lower-surface pressure distribution. Again no constraints were violated by the final design.

The quasi-64_1-212 airfoil used for adverse pressure gradient minimization was again used as the initial airfoil for the last lift maximization problem. Constraints on moment, volume, thickness, trailing-edge bluntness, and upper-surface pressure coefficients were imposed (see fig. 19). The final airfoil exhibits a modest increase in lift accompanied by a smaller pitching moment, an increased volume, a small peak upper-surface velocity, and a weaker adverse pressure gradient near the leading edge on the upper surface. Since this airfoil appears to be an attractive, high-lift airfoil, viscous calculations were carried out to further assess the validity of the inviscid theory and to explore the off-design characteristics. Figure 20 compares inviscid theory with viscous theory. Note that the pressure peak and adverse pressure gradient are lower when calculated by the viscous theory because of the displacement effects of the boundary layer. A reduction in lift coefficient and nosedown pitching moment is also noted. Generally, the agreement between the two theories is acceptable,

which shows again that meaningful low-speed airfoil design can be achieved with an inviscid theory. Figure 21 shows the effect of angle of attack on the aerodynamic characteristics of the final airfoil in figure 19. Note that the peak negative pressure coefficient is only -5 for $\alpha = 12°$. An empirical estimate based on the peak pressure and adverse pressure gradient indicates that the maximum lift coefficient is approximately 1.85. This estimate is a substantial improvement over the 64_1-212, which has a maximum lift coefficient of 1.5 at a Reynolds number of 6-million for the smooth surface condition (ref. 11). The final airfoil shown in figure 19 will be tested in the future to evaluate the validity of these predictions.

CONCLUDING REMARKS

A technique for the optimum design of low-speed airfoils was demonstrated. The results presented here show that the adverse pressure gradient and pitching moment can be reduced and the lift coefficient can be increased with an inviscid aerodynamic theory. Extending the technique to viscous drag minimization or lift/drag maximization is straightforward, depending on the availability of suitable aerodynamic programs that include boundary-layer effects. The procedure is an efficient, easy-to-use engineering approach to the design of airfoil sections.

The optimization problems considered here were performed on a CDC 7600 computer. A typical design problem used about three minutes of CPU time at a cost of approximately $55.

Further work is needed to develop equations for the airfoil geometry which allow greater flexibility in airfoil contour modification so that optimum design can be achieved for a greater variety of airfoils and isolated regions of the airfoil (e.g., leading or trailing edge) can be modified without altering the entire airfoil.

Ames Research Center
National Aeronautics and Space Administration
Moffett Field, Calif., 94035, January 14, 1975

APPENDIX

THEORETICAL CONSIDERATIONS

Aerodynamic Analysis

The aerodynamic analysis program uses a relaxation method to solve the nonlinear partial differential equation that governs the inviscid, potential fluid flow. The problem is solved by mapping the airfoil to the interior of a unit circle. Appropriate boundary conditions are specified on the airfoil surface and in the far field. The governing partial differential equation is of mixed elliptic-hyperbolic type and is solved by a mixed finite-difference, line relaxation algorithm. Solutions in which the flow is completely subsonic or transonic (mixed subsonic, supersonic) where both shock-free flows and embedded-shock flows are possible. (See ref. 8 for complete details of the theory and solution procedure.) The aerodynamic program was modified to fit the requirements of the optimization program, and the two programs were coupled to produce a single design optimization program.

During the optimization process, the aerodynamics of many different airfoils must be calculated. However, each airfoil is a small perturbation on the preceding airfoil and hence the flow characteristics of one airfoil provide a good initial estimate to start the calculation for the next airfoil. This process reduces the number of iterations required for convergence of the relaxation technique used to solve the fluid flow equation, thereby providing an efficient computational process.

The proposed procedure is not limited to two-dimensional airfoils. Lifting three-dimensional wings and axisymmetric bodies should be admissible problems to the proposed method.

Optimization Process

Numerous optimization algorithms are available in the literature, each with its own special mathematical characteristics. The basic concept common to each is that a sequence of improving designs is obtained, which leads to a final optimum solution that satisfies all imposed constraints unless such a design does not exist.

Mathematically stated, the optimization problem has the form:

$$\text{Minimize } OBJ = F(\bar{x}) \text{ subject to } G_j(\bar{x}) \leqslant 0\ , \quad j = 1,NCON$$

where $\bar{x}$ is a vector containing the design variables (in this case, the coefficients of the airfoil geometry function). When pitching moment is to be minimized, OBJ is the value of the moment coefficient, a highly nonlinear implicit function of the design variables. The term $G_j(\bar{x})$ defines the linear and nonlinear constraints on the design and $NCON$ is the total number of such constraints. For example, if the enclosed volume of the airfoil is required to be greater than or equal to a specified value, V_{min}, the corresponding constraint may be written in normalized form as

$$G(\bar{x}) = 1 - V(\bar{x})/V_{min} \leqslant 0$$

For the polynomial representation used for the airfoil shape, the above constraint is a linear function of the design variables. Other constraints considered include lift coefficient, pressure gradient, and pressure coefficient at some chordwise station on the airfoil.

For the airfoil design problem considered here, the upper and lower surfaces may be described, respectively, as

$$y_{us} = a_1\sqrt{x} + a_2P_2 + \ldots + a_6P_6$$

$$y_{\ell s} = b_1\sqrt{x} + b_2P_2 + \ldots + b_6P_6$$

where the coefficients $a_1 \ldots, a_6$ and $b_1 \ldots, b_6$ are the design variables contained in the $\bar{x}$ vector and $P_2, \ldots, P_6$ are Legendre polynomials. Non-negative thickness is ensured by imposing the linear constraints

$$y_{\ell s} - y_{us} \leqslant 0$$

at 50 chordwise stations. An example of the nonlinear constraints considered is the requirement that the lift coefficient be greater than some specified minimum, say C_L', so that

$$G(x) = 1 - C_L/C_L' \leqslant 0$$

If pitching moment is to be minimized, the objective function, OBJ, equals C_m. During the optimization process, the gradient

$$\nabla^T C_m = \frac{\partial C_m}{\partial a_1}, \ldots \frac{\partial C_m}{\partial a_6}, \frac{\partial C_m}{\partial b_1}, \ldots \frac{\partial C_m}{\partial b_6}$$

is required. Then if no constraints are active or violated (all $G_j(x) \leqslant 0$), the pitching moment is reduced by moving in the direction of steepest descent $-\nabla C_m$. If one or more constraints are active or violated (some $G_j(x) \geqslant 0$), a search is determined to reduce C_m subject to these constraints.

The general optimization procedure is to iteratively update the design so that at iteration q, $\bar{x}^q = \bar{x}^{q-1} + \beta\bar{s}^q$ where $\bar{s}$ is a vector direction in the n-dimensional design space and β is the distance of movement in direction $\bar{s}$. At iteration q, $\bar{s}$ is determined so that, for an arbitrarily small β, the objective function is decreased (usable direction) and no constraints are violated (feasible direction). If the initial design is not feasible (if it violates one or more constraints), a direction $\bar{s}$ is found that will overcome this constraint violation with minimal increase in the objective function. At any iteration, if one or more constraints are active or violated, the $\bar{s}$ vector is determined by the method of feasible directions (refs. 12 to 15). If no constraints are active, either a steepest descent or conjugate direction determined using the Fletcher-Reeves algorithm (refs. 16 and 17) is taken as the move direction. A constraint is defined to be active if

$$CT \leqslant G_j(\bar{x}) \leqslant CT$$

where CT is a small negative number used to identify near zero values of $G_j(x)$. This procedure is required because precise zero is seldom attainable numerically. A constraint is considered inactive if its value is less than CT and violated if it is greater than CT (CT is the "constraint tolerance").

The optimization algorithms are described in detail in references 12 through 17 and only a brief geometric interpretation is given here to identify the program requirements.

Consider the two-variable design space shown in figure 22 where an initial unconstrained design is prescribed at point A. At this point, the gradient of the objective function is calculated by a finite-difference computation using one-sided differences. The initial direction of movement from this point is the direction of steepest descent, $\bar{s} = -\nabla OBJ$. The parameter β is now determined so that OBJ is minimized or a constraint surface is encountered ($G_j(\bar{x}) = 0$) by moving in this direction. If the objective is nonlinear, subsequent directions are determined by the conjugate direction method (ref. 16) until a constraint surface is encountered (point B in fig. 22). At point B, the gradient of both the objective function and the active constraint(s) is required, again calculated by finite-difference computation. The feasible direction algorithm is used to determine $\bar{s}$. In this case, β is determined so that OBJ is minimized in direction $\bar{s}$, a new constraint is encountered or a currently active constraint is again encountered. If one or more constraints are violated (point C in fig. 22), as is often true for the initial design, a direction is determined that will point toward the feasible region with minimal increase in OBJ, based on gradients of the objective function and all active and violated constraints.

The optimum design program is segmented into three parts: the main program that initializes all design information; CONMIN, which performs the optimization; and the aerodynamic analysis routines to provide function and constraint evaluations. Figure 23 is a block diagram of the program organization. Optimization usually requires less than 10 design iterations. Gradient calculations using finite difference require n aerodynamic analyses per design iteration (n is the number of design variables). The move (one-dimensional search) in direction $\bar{s}$ requires an average of three analyses. Therefore, the maximum total number of aerodynamic analyses should seldom exceed $10n + 30$. The calculations described under Design Results and Discussion were carried out on a CDC 7600 computer. The majority of the results required about 3 minutes of CPU time, which corresponds to 50 to 150 separate flow calculations. Most of the relaxation calculations converged in 1 to 40 iterations.

REFERENCES

1. Stevens, W. A.; Goradia, S. H.; and Braden, J. A.: Mathematical Model for Two-Dimensional Multicomponent Airfoils in Viscous Flow. NASA CR-1843, 1971.

2. Bhateley, Ishwar, C.; and McWhirter, Jack W.: Development of Theoretical Method for Two-Dimensional Multi-Element Airfoil Analysis and Design. AFFDL-TR-72-96, August 1972.

3. McGhee, Robert J.; and Beasley, William D.: Low-Speed Aerodynamic Characteristics of a 17 Percent Thick Airfoil Section Design for General Aviation Applications. NASA TN D-7428, December 1973.

4. Liebeck, R. H.: A Class of Airfoils Designed for High Lift in Incompressible Flow. Journal of Aircraft, Vol. 10, no. 10, October 1973, pp. 610–617.

5. Strand, T.: Exact Method of Designing Airfoils With Given Velocity Distribution in Incompressible Flow. Journal of Aircraft, vol. 10, no. 11, November 1973, pp. 651–659.

6. Hicks, Raymond M.; Murman, Earll M.; and Vanderplaats, Garret N.: An Assessment of Airfoil Design by Numerical Optimization. NASA TM X-3092, 1974.

7. Vanderplaats, Garret N.: CONMIN: A Fortran Program for Constrained Function Minimization. User's Manual, NASA TM X-62,282, 1973.

8. Jameson, Antony: Transonic Flow Calculations for Airfoils and Bodies of Revolution. Grumman Aerospace Corp. Aerodynamics Rept. 390-71-1, December 1971.

9. Wortman, F. X.: Design of Airfoils With High Lift at Low and Medium Subsonic Mach Numbers. Fluid Dynamics of Aircraft Stalling. AGARD Conference Proceedings CP-102, April 1972, pp. 7-1–7-9.

10. McCullough, G. B.; and Gault, D. E.: Examples of Three Representative Types of Airfoil-Section Stall at Low Speed. NACA TN 2502, Sept. 1951.

11. Abbott, I. H.; von Doenhoff, A. E.; and Stivers, L. S., Jr.: Summary of Airfoil Data. NACA Report No. 824, 1945.

12. Zoutendijk, K. G.: Methods of Feasible Directions; A Study in Linear and Non-Linear Programming. (Thesis) Elsevier Publishing Co., Amsterdam, 1960.

13. Vanderplaats, Garret N.; and Moses, Fred: Structural Optimization by Methods of Feasible Directions. Computers and Structures, vol. 3, no. 4, July 1973, pp. 739–755.

14. Kowalik, J. S.: Feasible Direction Methods. Structural Design Applications of Mathematical Programming Technique, AGARDograph 149, Ch. 7, February 1971.

15. Tocher, J. L.; and Karnes, R. N.: The Impact of Automated Structural Optimization on Actual Design. AIAA Paper 71-361, April 1971.

16. Fletcher, R.; and Reeves, C. M.: Functional Minimization by Conjugate Gradients. Computer Journal, vol. 7, no. 2, July 1964, pp. 149–154.

17. Fox, Richard L.: Optimization Methods for Engineering Design. Addison-Wesley, Reading, Mass., 1971.

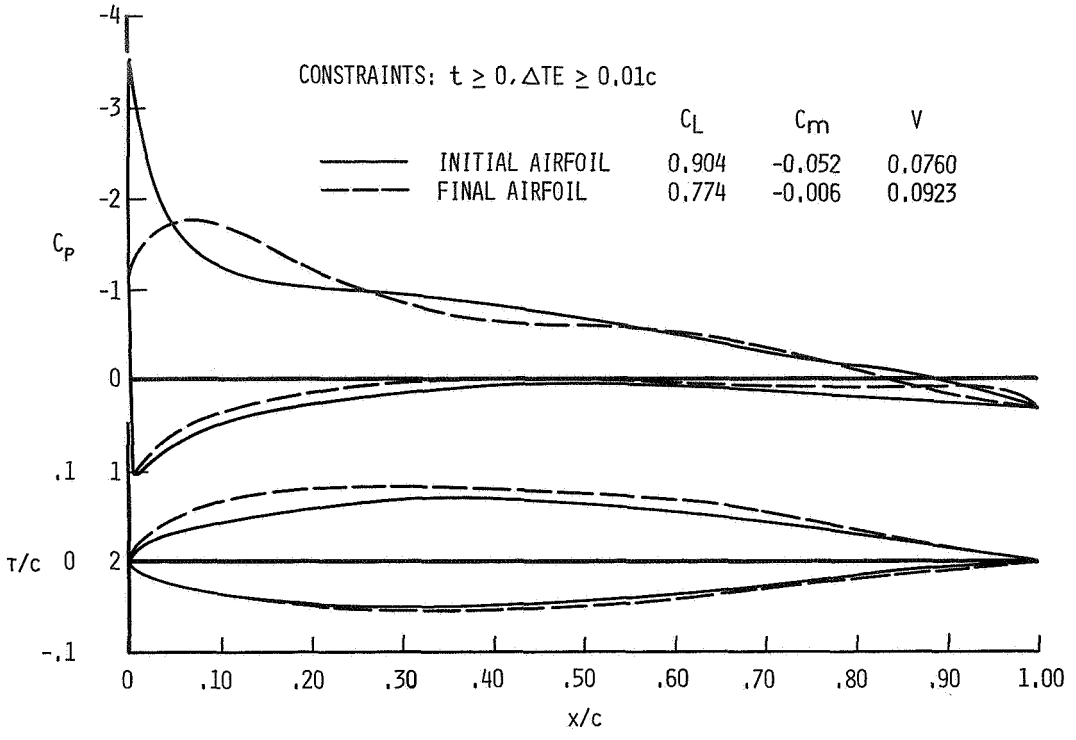

Figure 1.– Upper surface adverse pressure gradient minimization; $M = 0.1$, $\alpha = 6°$.

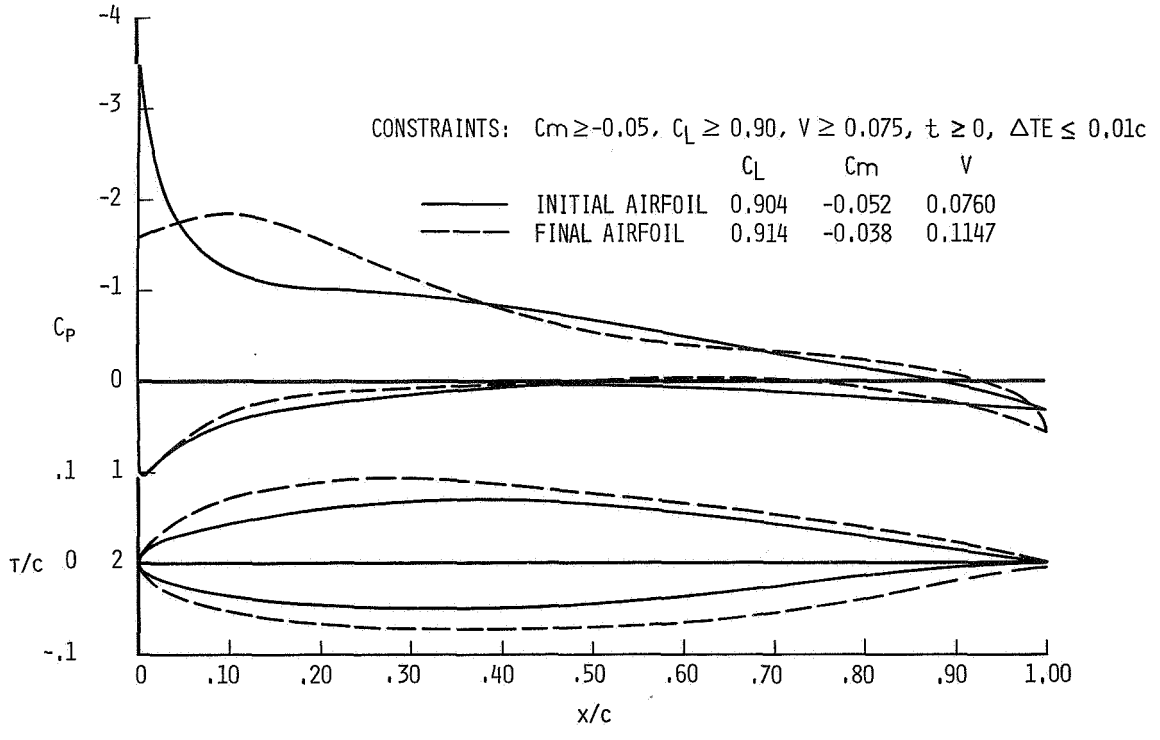

Figure 2.– Upper surface adverse pressure gradient minimization; $M = 0.1$, $\alpha = 6°$.

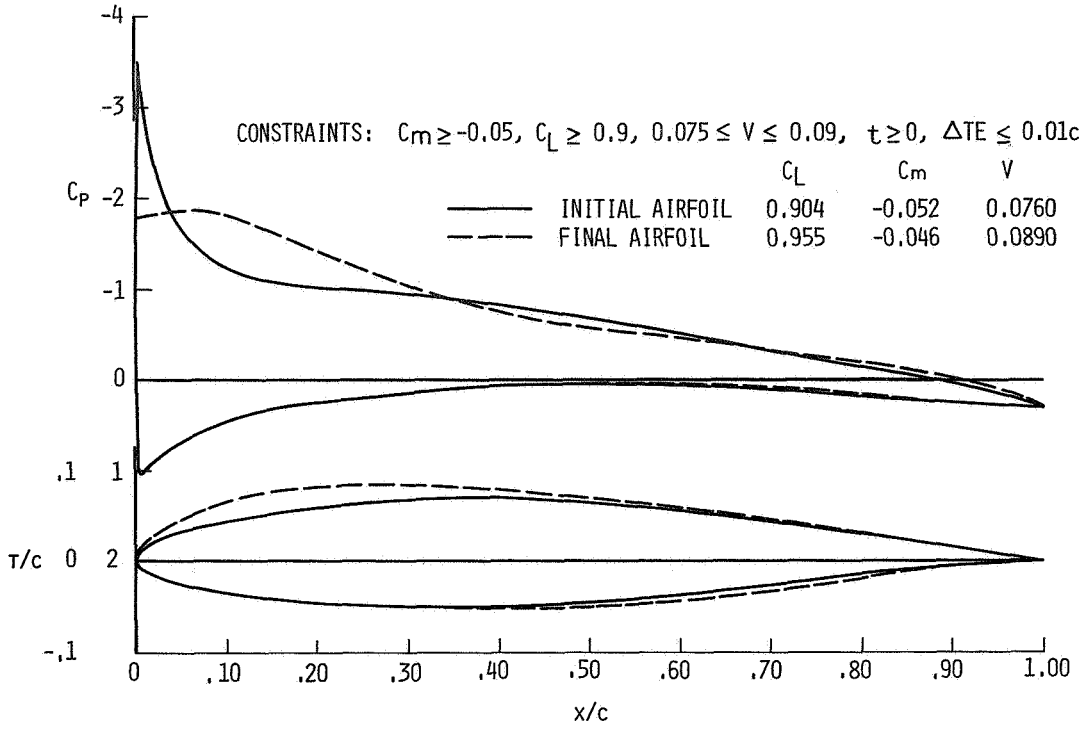

Figure 3.– Upper surface adverse pressure gradient minimization; $M = 0.1$, $\alpha = 6°$.

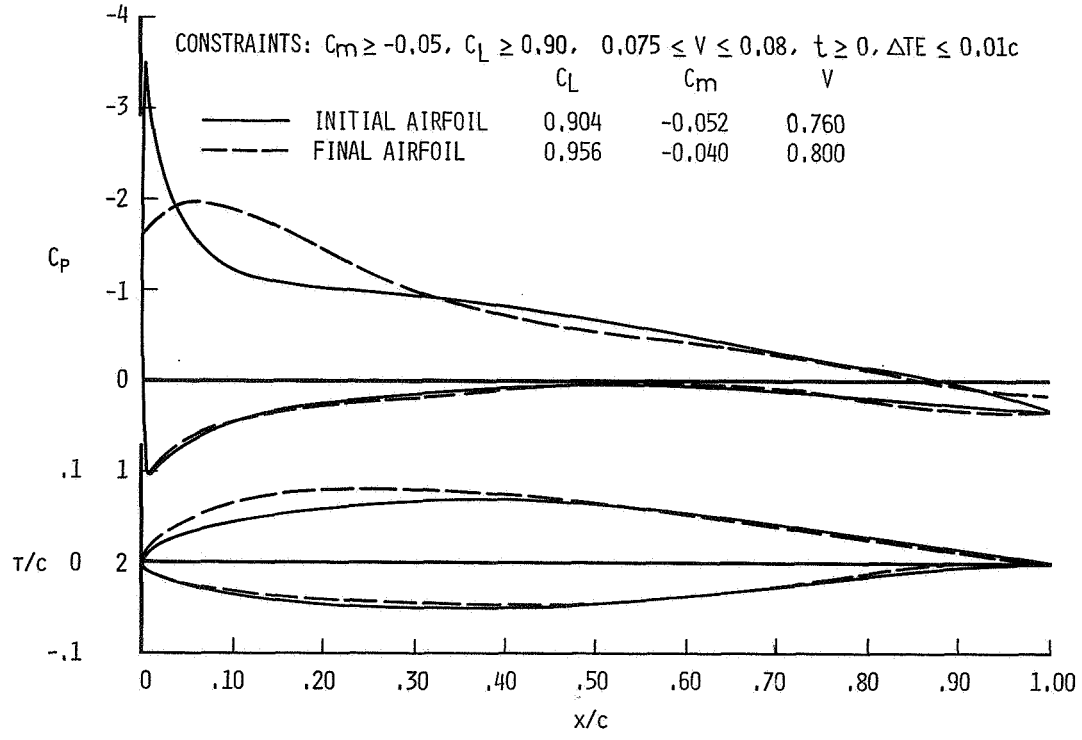

Figure 4.– Upper surface adverse pressure gradient minimization; $M = 0.1$, $\alpha = 6°$.

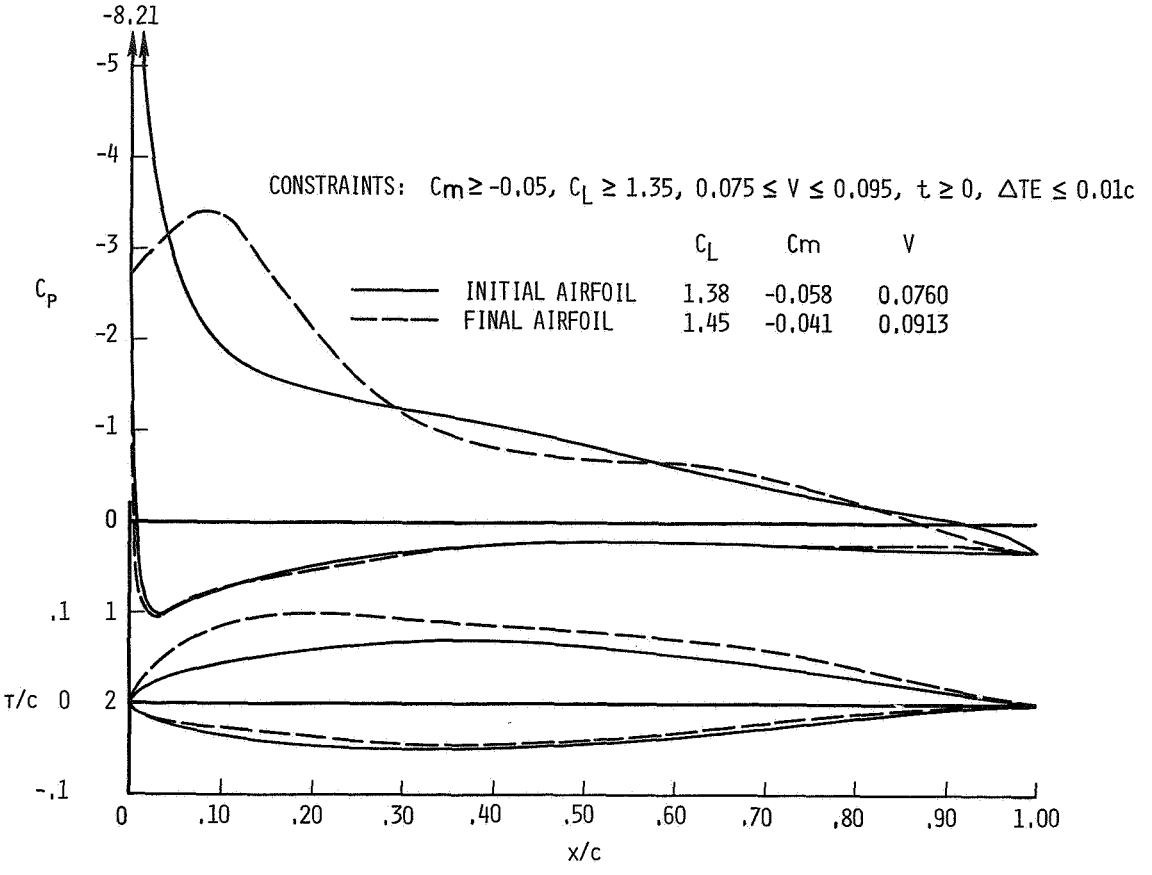

Figure 5.– Upper surface adverse pressure gradient minimization; $M = 0.1$, $\alpha = 10°$.

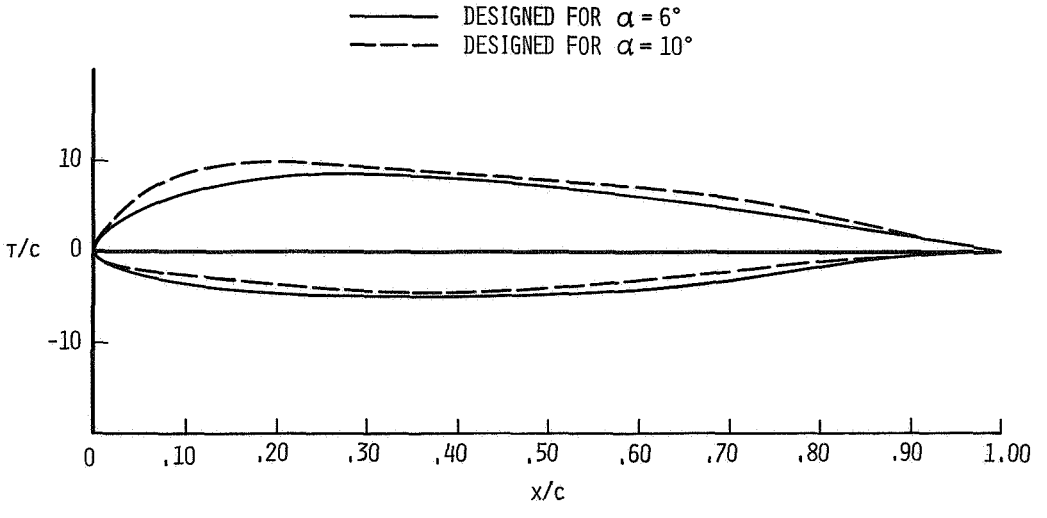

Figure 6.– Comparison of airfoil contours designed for different angles of attack; $M = 0.1$.

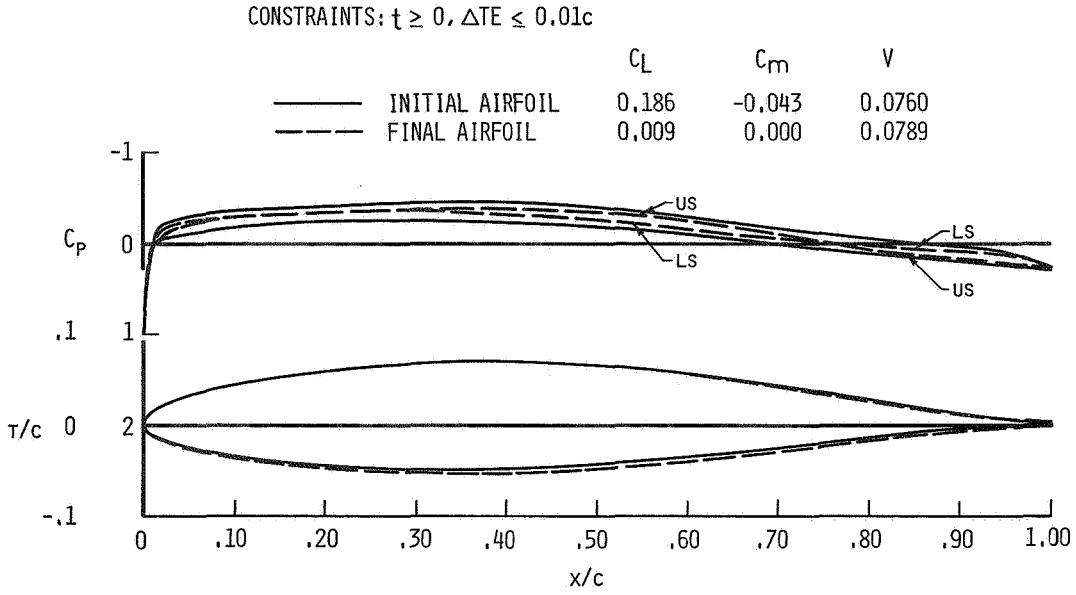

Figure 7.– Pitching-moment minimization; $M = 0.1$, $\alpha = 0°$.

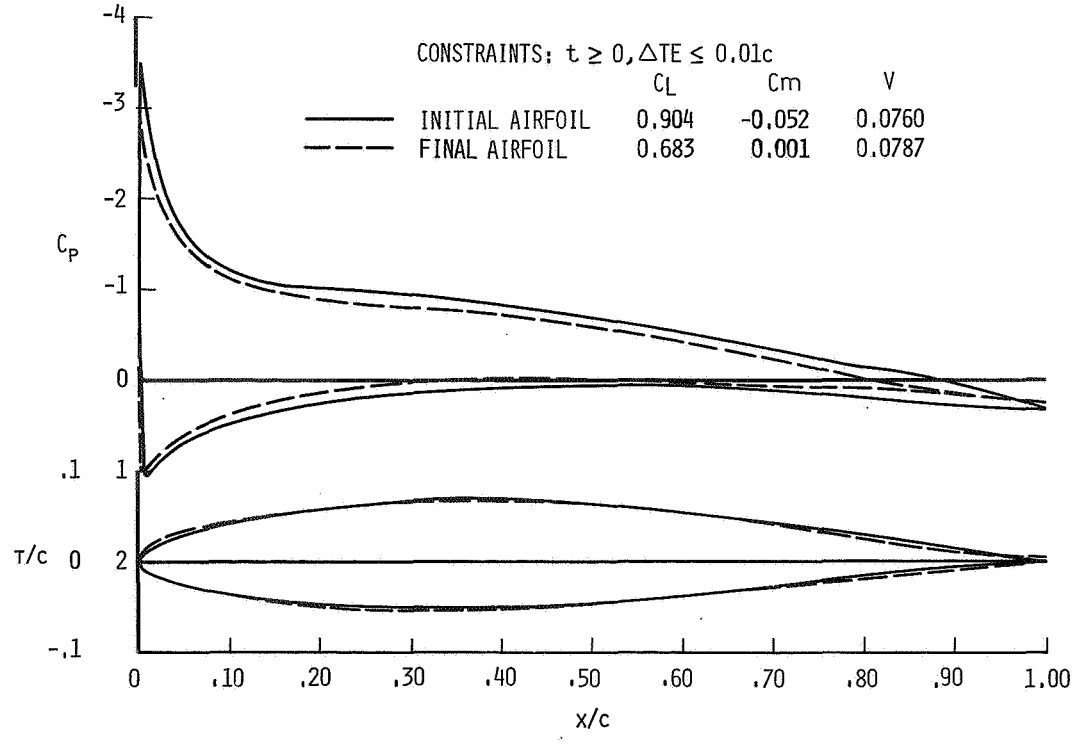

Figure 8.– Pitching-moment minimization; $M = 0.1$, $\alpha = 6°$.

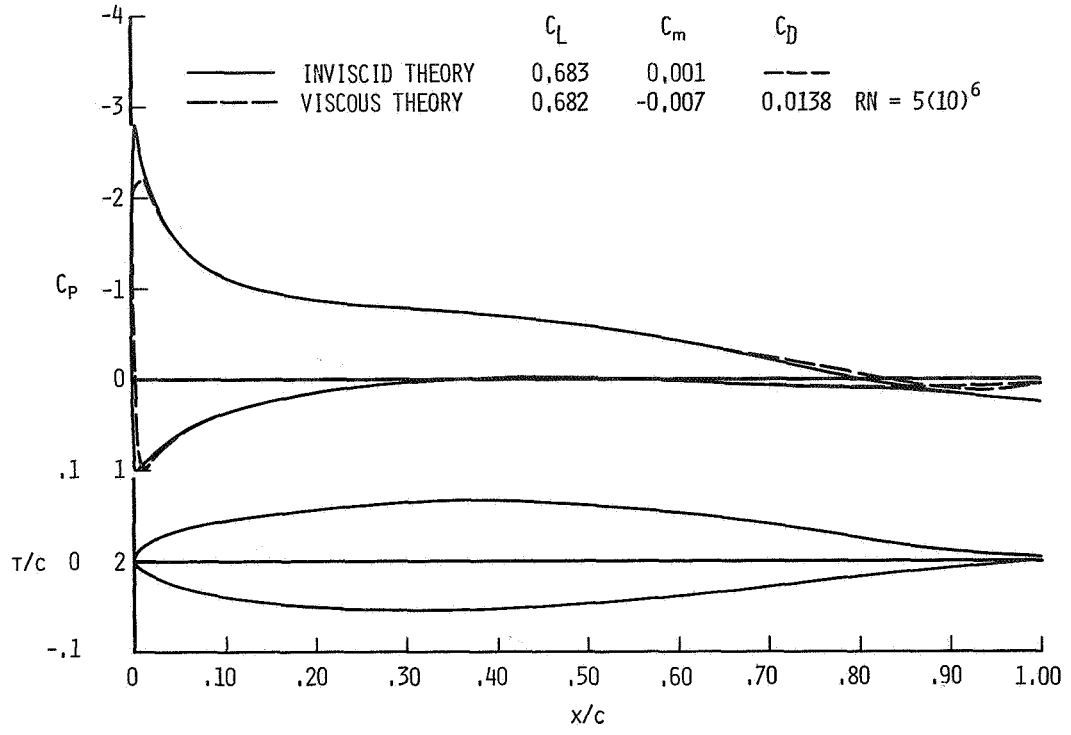

Figure 9.– Comparison of inviscid theory with viscous theory for the final airfoil in figure 8; $M = 0.1, \alpha = 6°$.

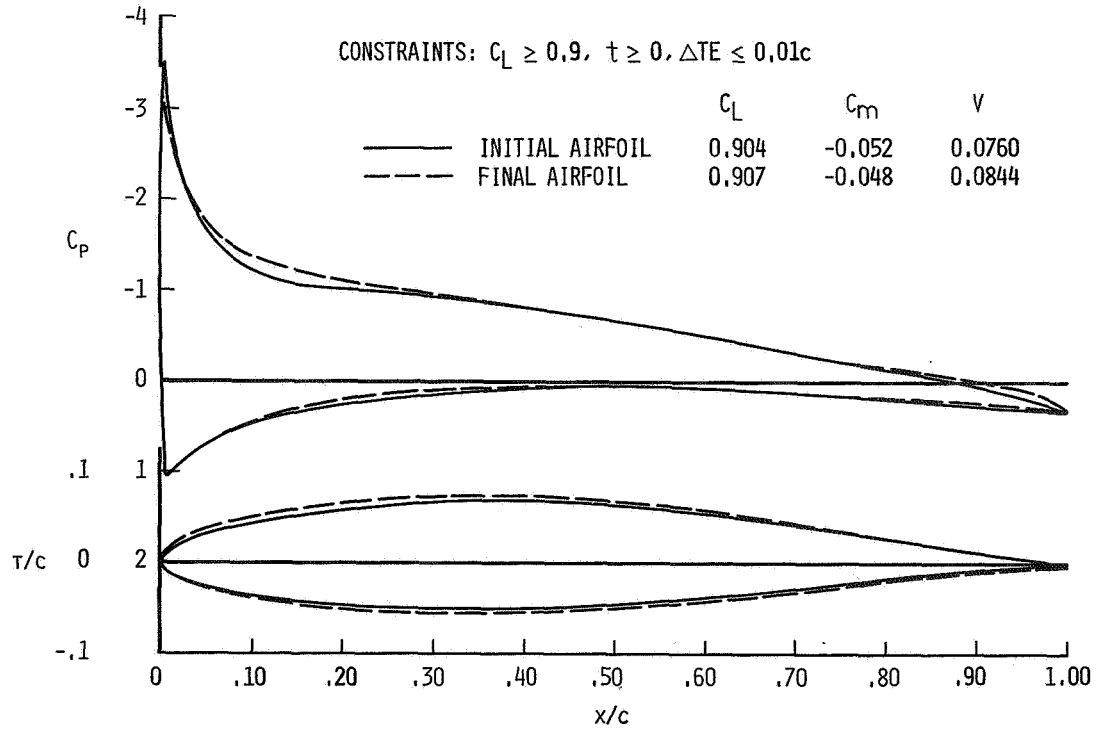

Figure 10.– Pitching-moment minimization; $M = 0.1$, $\alpha = 6°$.

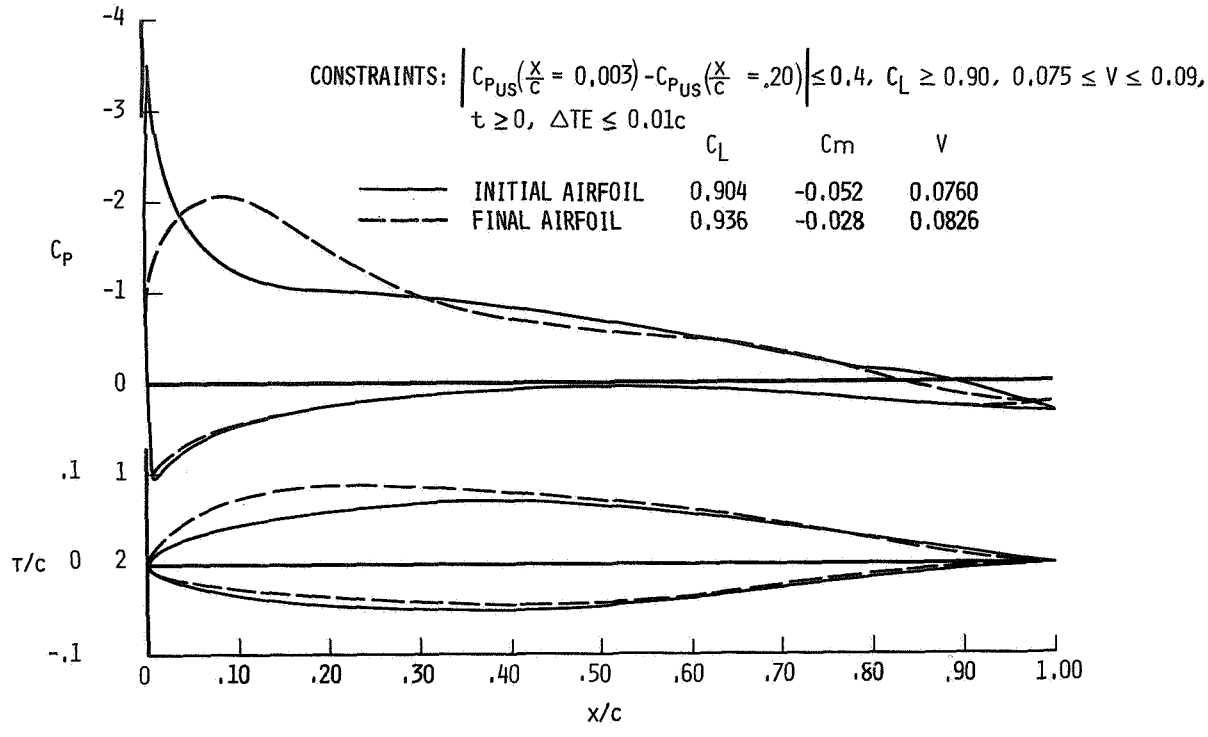

Figure 11.– Pitching-moment minimization; $M = 0.1$, $\alpha = 6°$.

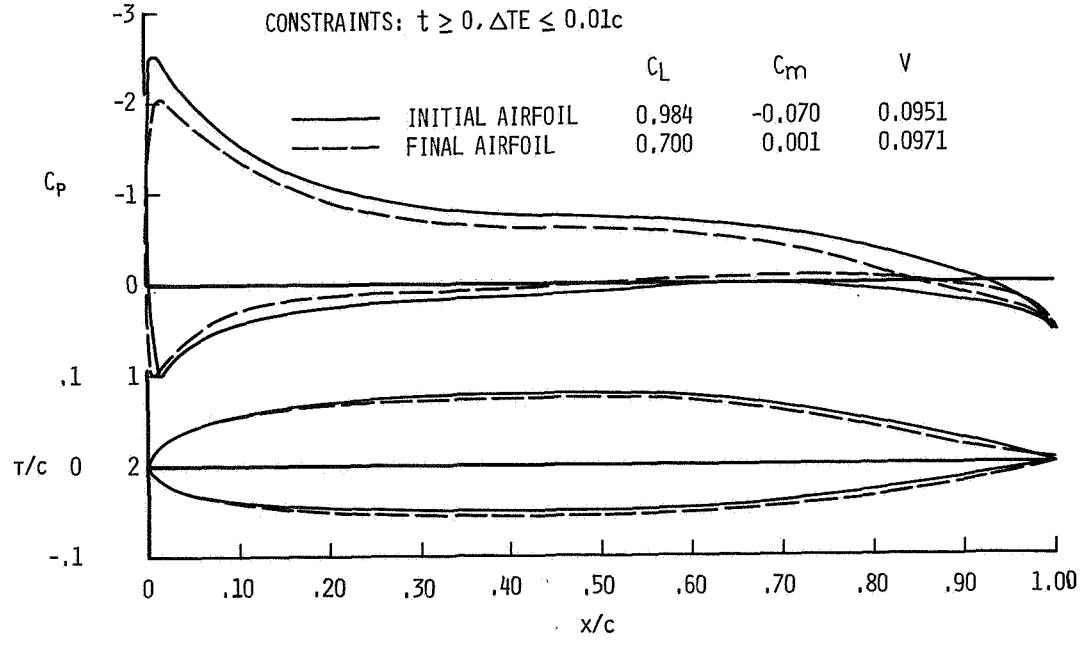

Figure 12.– Pitching-moment minimization; $M = 0.1$, $\alpha = 6°$.

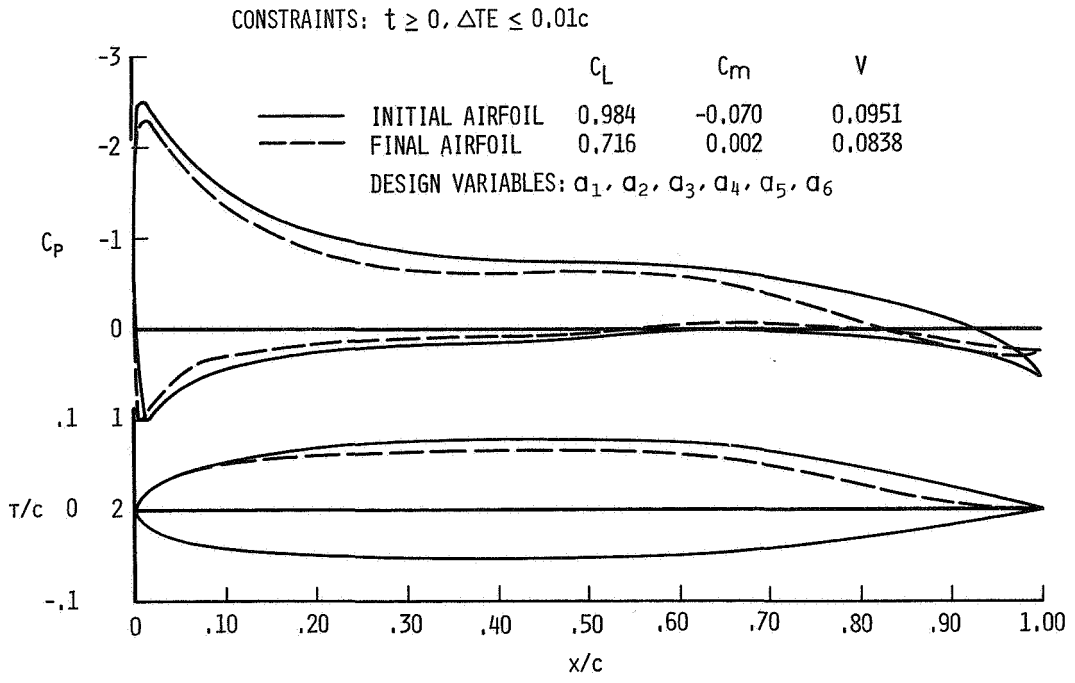

Figure 13.– Pitching-moment minimization; $M = 0.1$, $\alpha = 6°$.

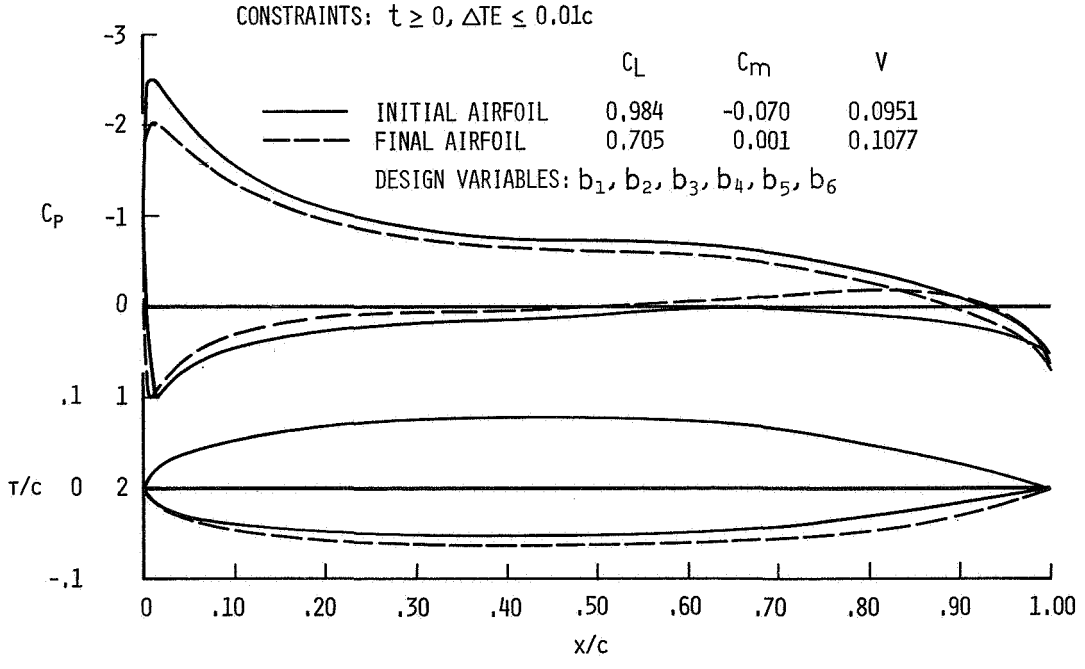

Figure 14.– Pitching-moment minimization; $M = 0.1$, $\alpha = 6°$.

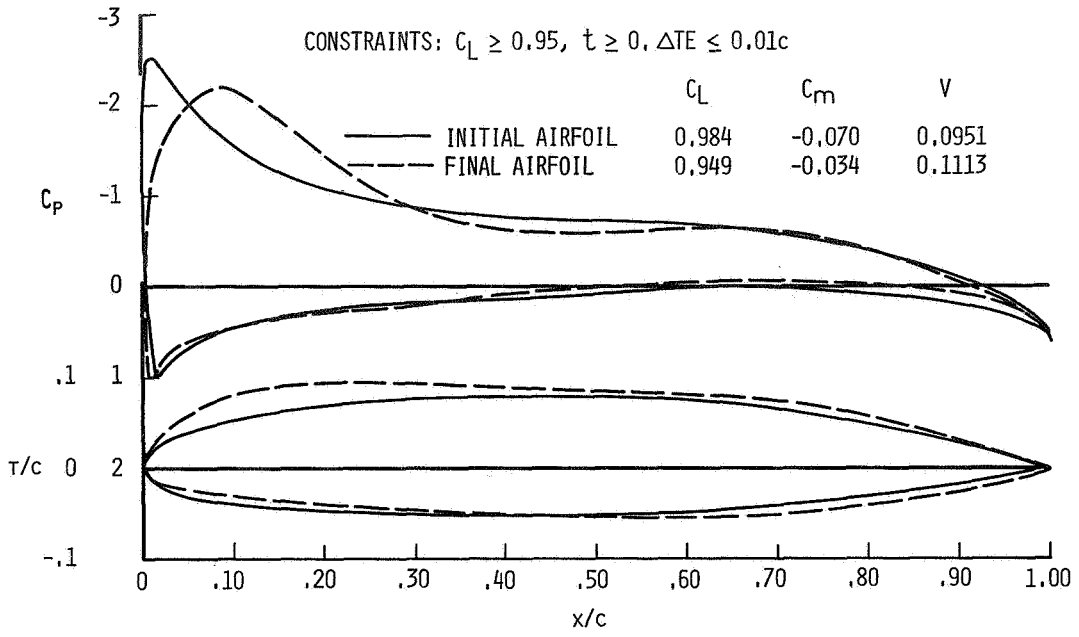

Figure 15.– Pitching-moment minimization; $M = 0.1$, $\alpha = 6°$.

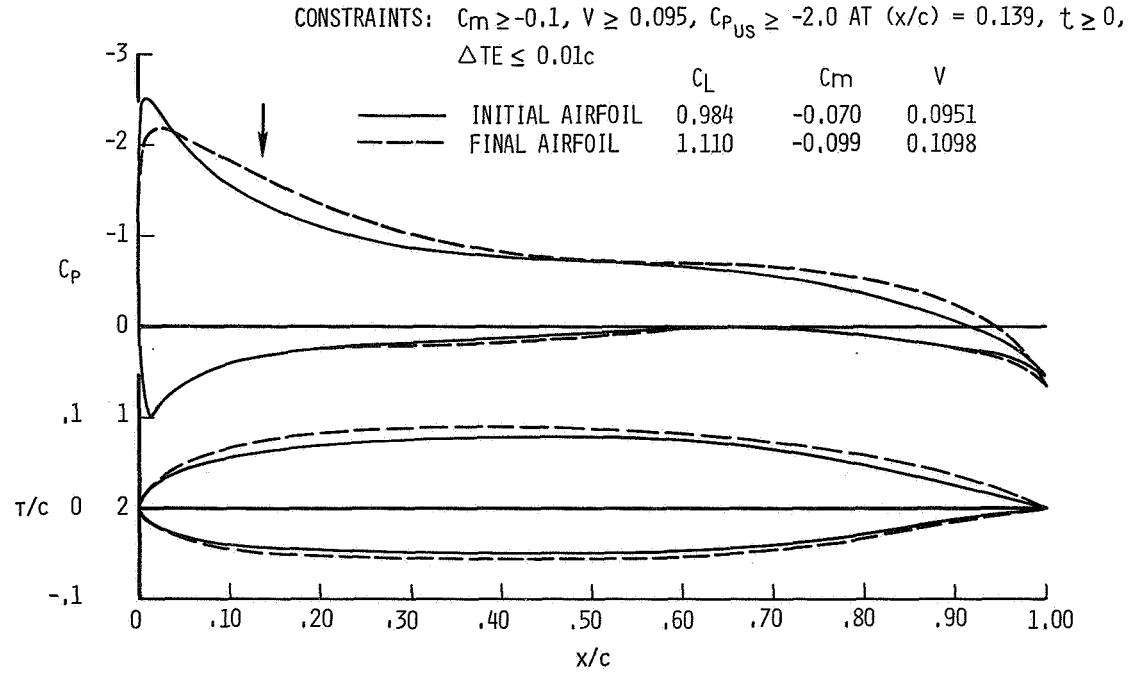

Figure 16.– Lift maximization; $M = 0.1$, $\alpha = 6°$.

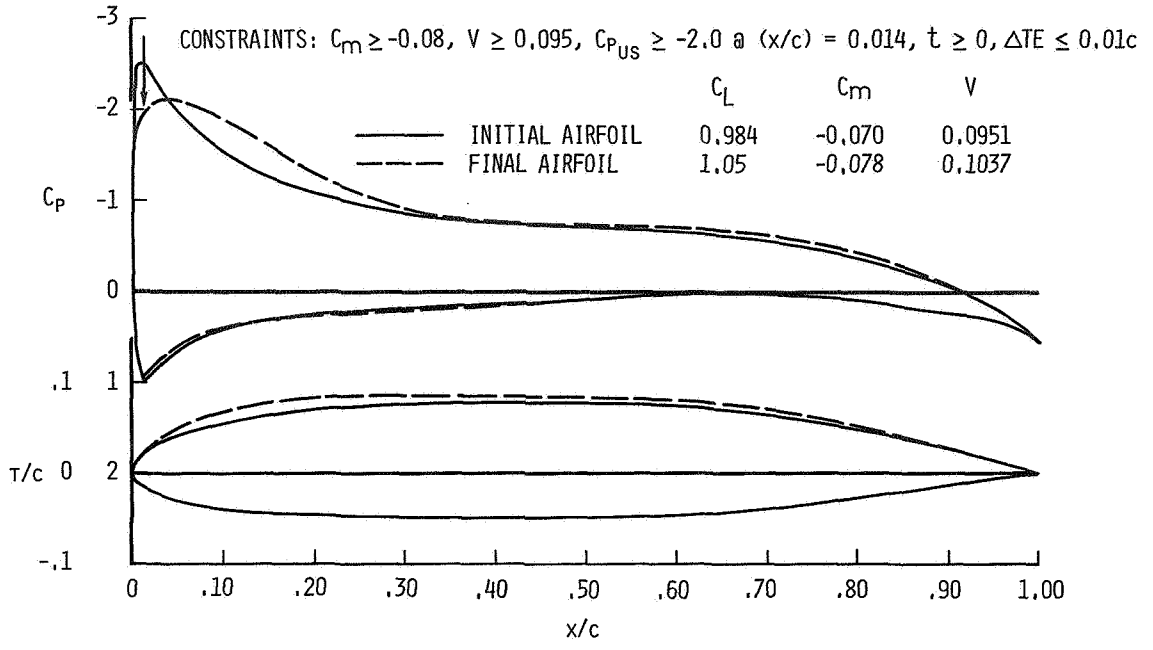

Figure 17.– Lift maximization; $M = 0.1$, $\alpha = 6°$.

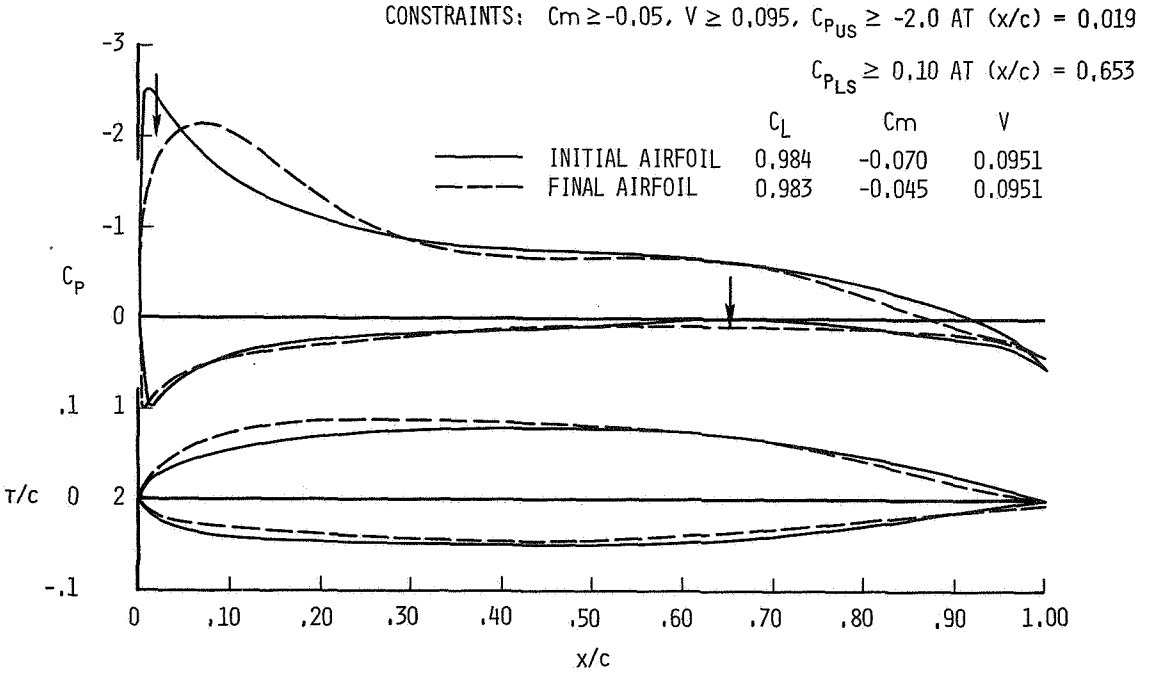

Figure 18.– Lift maximization; $M = 0.1$, $\alpha = 6°$.

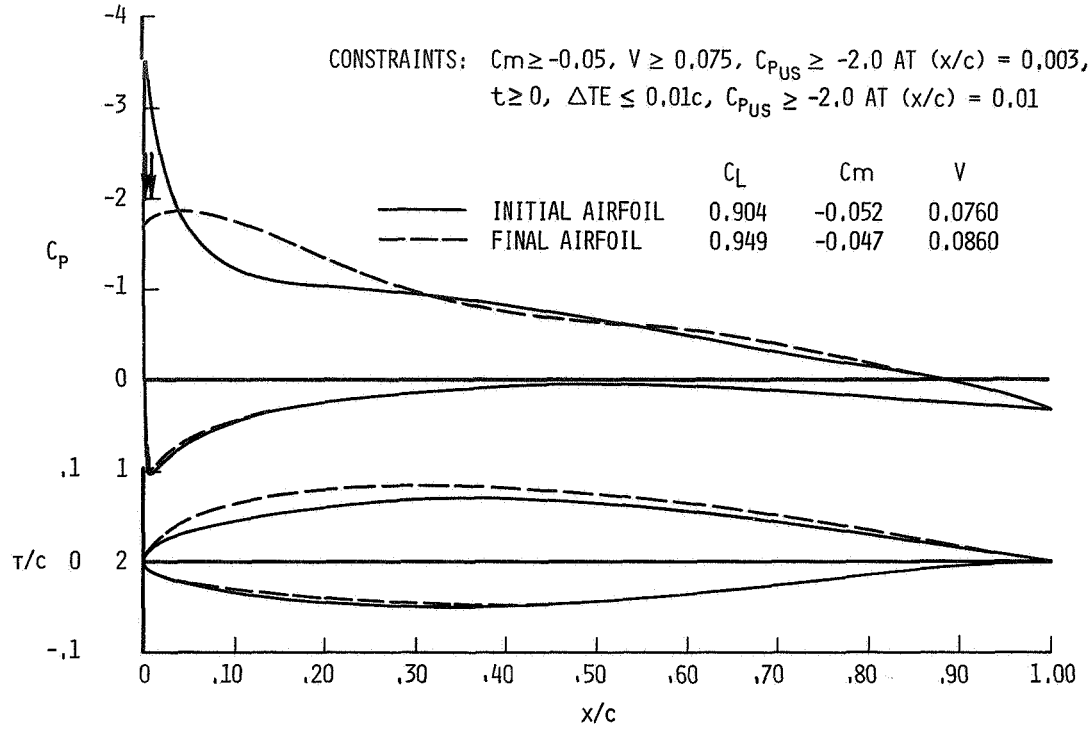

Figure 19.– Lift maximization; $M = 0.1$, $\alpha = 6°$.

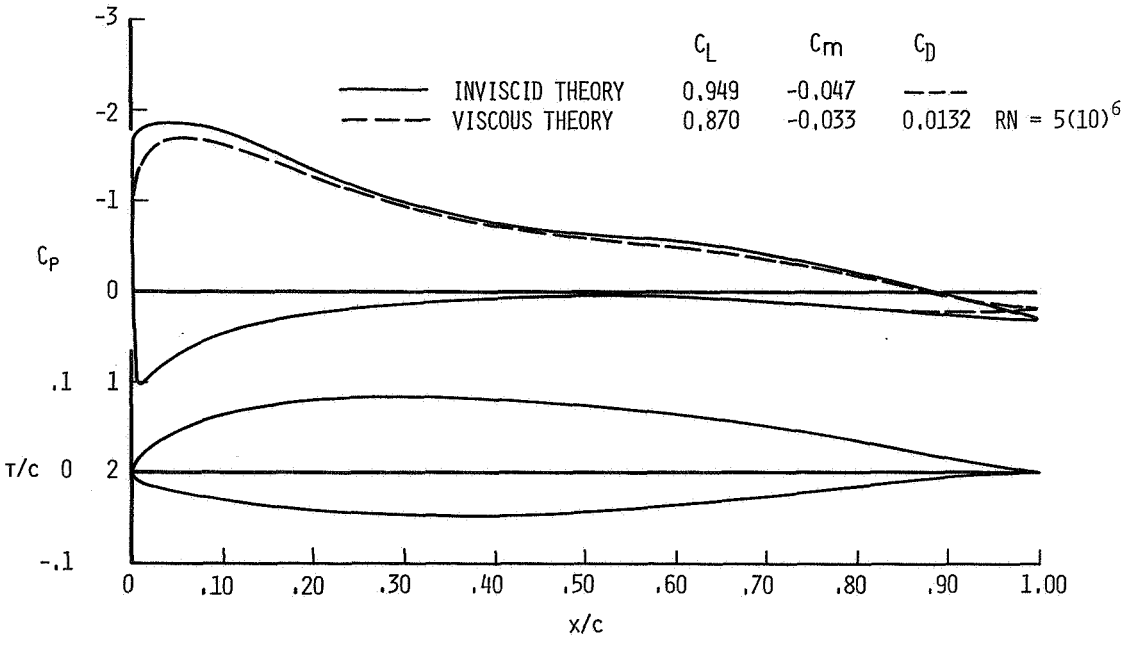

Figure 20.– Comparison of inviscid theory with viscous theory for the final airfoil in figure 19; $M = 0.1, \alpha = 6°$.

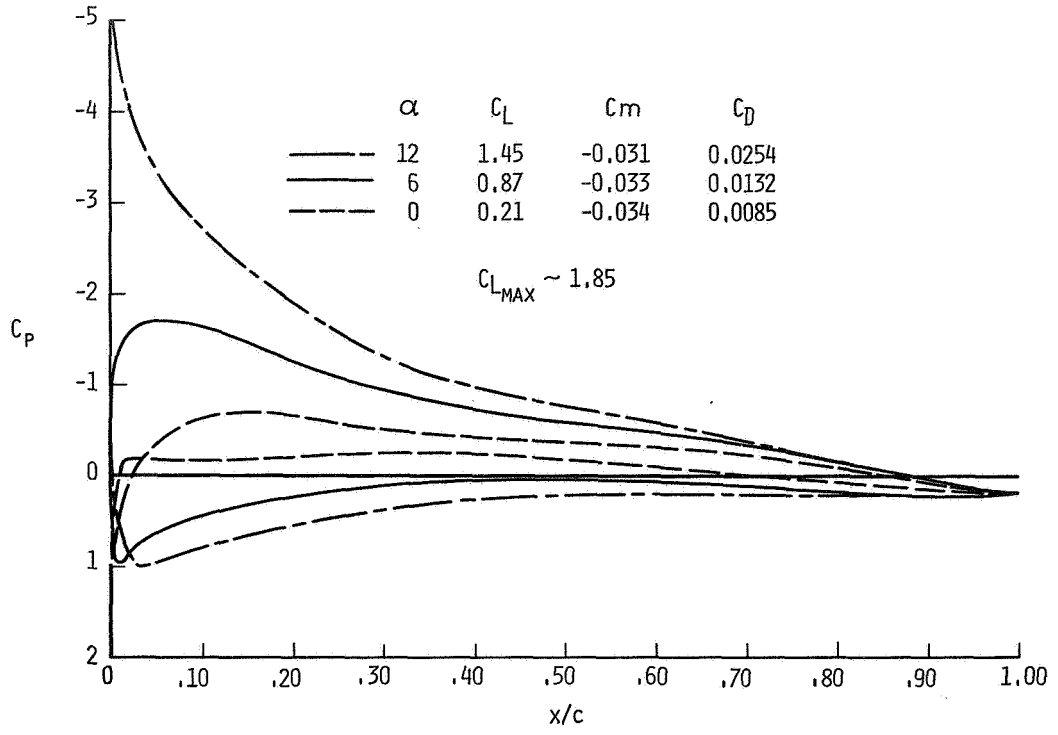

Figure 21.– Angle of attack effect for the final airfoil in figure 19; $M = 0.1$, $RN = 5(10)^6$.

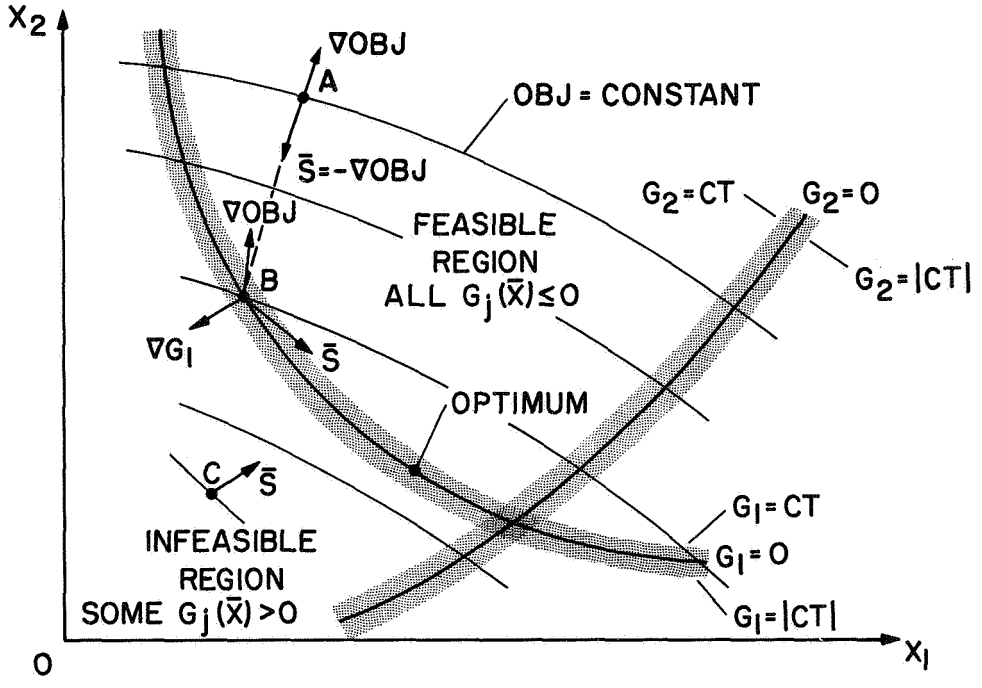

Figure 22.– Two-variable design space.

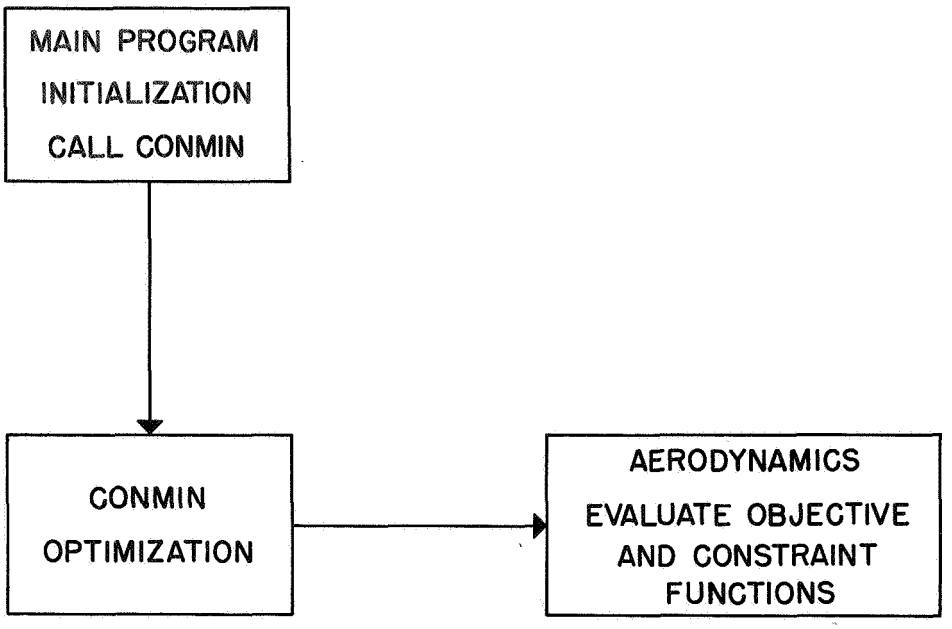

Figure 23.– Program organization.

SPECIAL FOURTH-CLASS RATE
BOOK

"The aeronautical and space activities of the United States shall be conducted so as to contribute . . . to the expansion of human knowledge of phenomena in the atmosphere and space. The Administration shall provide for the widest practicable and appropriate dissemination of information concerning its activities and the results thereof."

—National Aeronautics and Space Act of 1958

NASA SCIENTIFIC AND TECHNICAL PUBLICATIONS

TECHNICAL REPORTS: Scientific and technical information considered important, complete, and a lasting contribution to existing knowledge.

TECHNICAL NOTES: Information less broad in scope but nevertheless of importance as a contribution to existing knowledge.

TECHNICAL MEMORANDUMS: Information receiving limited distribution because of preliminary data, security classification, or other reasons. Also includes conference proceedings with either limited or unlimited distribution.

CONTRACTOR REPORTS: Scientific and technical information generated under a NASA contract or grant and considered an important contribution to existing knowledge.

TECHNICAL TRANSLATIONS: Information published in a foreign language considered to merit NASA distribution in English.

SPECIAL PUBLICATIONS: Information derived from or of value to NASA activities. Publications include final reports of major projects, monographs, data compilations, handbooks, sourcebooks, and special bibliographies.

TECHNOLOGY UTILIZATION PUBLICATIONS: Information on technology used by NASA that may be of particular interest in commercial and other applications. Publications include Tech Briefs, Technology Utilization Reports and Technology Surveys.

Details on the availability of these publications may be obtained from:

SCIENTIFIC AND TECHNICAL INFORMATION OFFICE

NATIONAL AERONAUTICS AND SPACE ADMINISTRATION

Washington, D.C. 20546